55th AAVLD Diagnostic Pathology Slide Session

American Association of Veterinary Laboratory Diagnosticians
Greensboro, North Carolina
Saturday, October 20, 2012
3:30-6:00 PM

2012 AAVLD Diagnostic Pathology Slide Seminar Presenters

Case #	Page #	Presenter	Species	Organ	Diagnosis	Institution
1	3	Tucker	Horse	Placenta	Equine allantoic adenomatous hyperplasia	NCVDLS
2	4	Fitzgerald	Trinket snake	Heart, kidney	Disseminated mycobacteriosis	MSU
3	5	Burrough	Pig	Skin, kidney, spleen	Erysipelas	ISUVDLS
4	6	Uzal	Goat	Brain	Focal symmetrical encephalomalacia	UCDavis
5	7	Loynhachan	Dog	Conjunctiva	Ligneous conjuctivitis	UK VDL
6	8	Pinkerton	Dog	Lung	Pulmonary carcinosarcoma	Univ Wisc
7	9	Tobias	Cat	Lung	Hypereosinophilic syndrome	NCSU CVM
8	10	Craig	Cat	Heart	Feline endomyocarditis	UTCVM
9	11	Scholes	Calf	Spinal cord	In utero Schmallenberg virus	AHVLA
10	12	Boone	Avian		Pararenal myelolipomas	NCSU CVM
11	13	Caesar	Dog	Intestine	Salmonella newport and parvovirus	NCVDLS
12	14	Bernard	Dog	Lung	Canine distemper and adenovirus	UTCVM
13	15	Hayes	Dog	Placenta	Brucella canis abortion	OH ADDL
14	16	Almes	Pig	Spinal cord	Selenium toxicosis	KSVDL
15	17	Johnson	Dog	Brain	Fourth ventricular cystic mass	UMVMDL
16	18	Salas	Dog	Skin	Exfoliative dermatitis	UNebr
17	19	Ilha	Hamster	Skin, muscle and bone	Bacterial pseudomycetoma	UGA/Tifton

55th AAVLD Diagnostic Pathology Slide Seminar

Case #1

Adenomatous Hyperplasia of Equine Allantoic Epithelium

Alison Tucker, David Drum

North Carolina Veterinary Diagnostic Laboratory System, Raleigh, NC

Signalment: 4 year old Hanoverian mare

Clinical History: On 04/07/2012 an equine placenta was dropped off at the NC Western Animal Disease Diagnostic Laboratory for evaluation because it looked "funny". According to the history provided, the mare was a maiden mare, bred with cooled shipped semen, one cycle, and ovulated Saturday, May 8, 2011. She foaled April 6th, 2012 (334 days gestation). The foal was normal at birth, transiently developed diarrhea but recovered with treatment and has been normal since. The mare developed a purulent vaginal discharge post partum. *Pantoea (Enterobacter) agglomerans* was isolated from a uterine sample. The mare responded to treatment and a follow-up culture 8 weeks post partum was negative.

The allantoic surface of the placenta contains multiple coalescing, 12 cm and smaller, firm, umbilicated exophytic masses that are distributed along the umbilical blood vessels. On cut surface the masses have variably sized cystic spaces that contain clear to opaque material. The chorionic surface is coated with an opaque red to tan exudate.

A hematoxylin and eosin stained section of allantois is included in the slide set.

Microscopic Description: An exophytic nodule from the allantois contains irregularly shaped and variably sized cystic structures. The lumens contain globular homogeneous eosinophilic to basophilic material, neutrophils, macrophages, sloughed cells with karyorrhexis, and erythrocytes. The cystic structures are lined by a single layer of attenuated cuboidal to tall columnar epithelium supported by a collagenous stroma. Where columnar, cells have abundant eosinophilic cytoplasm and basally placed nuclei. Pleomorphism is marked. Surface epithelium is columnar and there is occasional contiguity with superficial cystic structures. Vessels in the stroma are congested. There are moderate disseminated infiltrates of lymphocytes, plasma cells, macrophages and fewer neutrophils and fibroblasts.

Diagnosis: Placenta: Adenomatous hyperplasia of allantoic epithelium

Comment: Adenomatous hyperplasia of allantoic epithelium has been reported in the literature in association with chronic placental lesions, primarily bacterial or fungal placentitis. Nocardioforms and *E coli* were most commonly isolated in the report by Hong, et al. Clinical cases include late term abortion, early neonatal clinical disease, and asymptomatic foals.

Pantoea (*Enterobacter) agglomerans* is a Gram negative aerobic bacillus, isolated from plants, soil and fecal material, that has been associated with placentitis and late term abortion in horses.

References:

Hong, CB, et al. Adenomatous hyperplasia of equine allantoic epithelium. Vet Pathol 30:171-175 (1993).

Hong, CB, et al. Etiology and pathology of equine placentitis. J Vet Diagn Invest 5:56-63 (1993).

McEntee, M, et al. Adenomatous dysplasia of the equine allantois. Vet Pathol 25:387-389 (1988).

Shivaprasad, HL, et al. Cystic adenomatous hyperplasia of the equine allantois: a report of eight cases. J Vet Diagn Invest 6:107-110 (1994).

Case #2

A Case of Disseminated Mycobacteriosis in a Assam Trinket Snake

Scott D. Fitzgerald[1], Steven R. Bolin[1] and Sarah Woodhouse[2]

[1]Diagnostic Center for Population and Animal Health, Michigan State University,

Lansing, MI

[2]Detroit Zoological Society, Royal Oak, MI

An adult male Assam trinket snake (*Elaphe frenata*) was found dead in its enclosure without premonitory signs. On gross necropsy, a 1.5x0.5x0.5 cm firm mass was present in the right craniolateral epaxial musculature. The lung was severely and diffusely thickened. The ventricular wall of the heart was mottled. The stomach contained a single transmural mass.

Histologically, there were disseminated granulomatous infiltrates composed of numerous macrophages, lymphocytes, and rare heterophils and multinucleated giant cells. Many macrophages contained large clear intracytoplasmic vacuoles. This granulomatous infiltrate formed a large transmural mass in the stomach; multiple foci within the myocardium and extending into the pericardial adipose tissue; formed multifocal to coalescing nodules replacing much of the parenchyma of the liver; formed multifocal subcapsular nodules in the kidney; diffusely infiltrated the connective tissues in the neck surrounding both the trachea and thyroid; and formed a locally extensive mass replacing the myofibers of the craniolateral epaxial muscles. Fite-Farracho acid-fast stains revealed numerous intracytoplasmic acid-fast bacilli within macrophages, often clustered within the cytoplasmic vacuoles seen on H&E.

The fresh lung and liver samples were tested by PCR for the hsp65 gene of Mycobacteria and were strongly positive. PCR amplicons were sequenced, and the mycobacteria were identified by BLAST analysis as *Mycobacterium haemophilum*. *M. haemophilum* has been reported several times as causing disease in reptiles, including one report of pneumonia in a royal python, and additional granulomatous infections in a turtle and a snake. A recent review on *M. haemophilum* indicated that it is an emerging opportunistic infection in immunocompromised humans worldwide. This organism was first named in 1978, is believed to be a ubiquitous environmental opportunistic pathogen. It grows best in vitro between 30 to 32^{o}C, making it an ideal pathogen for reptiles and for cutaneous infections in humans. In summary, *M. haemophilum* is an organism of low virulence, and serves as an opportunistic infection in immunocompromised humans and poikilotherms such as snakes and turtles. It should be included in the differential for disseminated granulomatous disease in reptiles.

References:

Hernandez-Divers SJ, Shearer D: Pulmonary Mycobacteriosis Caused by *Mycobacterium haemophilum* and *M. marinum* in a Royal Python. J. Amer. Vet. Med. Assoc. 220:1661-1663, 2002.

Soldati G, Lu ZH, Vaughn L, Polkinghorne A, Zimmerman DR, Huder JB, Pospischil A: Detection of Mycobacteria and Chlamydiae in Granulomatous Inflammation of Reptiles: A Retrospective Study. Vet. Pathol. 41:388-397, 2004.

Case #3

Acute Swine Erysipelas in Recently Weaned Pigs

Eric R. Burrough, Kent J. Schwartz

Iowa State University Veterinary Diagnostic Laboratory, Ames, IA

Signalment: 3-week-old pigs just weaned from the sow farm

Clinical History: Per submitting veterinarian, five hundred 20-day-old pigs were weaned early in the morning and arrived via truck at the nursery in the afternoon. At least 50 were reported with severe purple discoloration of the ears and rumps when unloaded at the nursery, with several piglets found dead at time of arrival. Gross lesions at necropsy included severe, multifocal, dark purple discoloration and swelling of the skin of the ears, coronary bands, and posterior aspects of the thighs which varied from irregularly polygonal to confluent. One of three pigs had sloughed the lateral hoof of its right hind leg, and another pig had several 4 mm diameter vesicles on the internal surface of the ear and two similar vesicles on the roof of its mouth. Petechial and ecchymotic hemorrhages were noted beneath the capsule of kidneys of all pigs, and one of three pigs had marked congestion and hemorrhage at the corticomedullary junction. Marked splenomegaly was noted in one pig. A 4 μm, H&E stained slide with sections of haired skin, kidney, and spleen is included in the slide set.

Microscopic Description:

- Haired skin: Superficial dermal vessels are diffusely congested and multifocal small vessels and capillaries are occluded by fibrin thrombi. There is marked perivascular to diffuse hemorrhage in some areas and multifocal blood vessels in the mid to deep dermis have thickened and hyalinized walls, are lined by plump endothelia, have few too many transmigrating neutrophils, and occasionally contain luminal thrombi. The mid to deep dermis is variably infiltrated by neutrophils and multifocal lymphatics are ectatic and contain fibrin thrombi. There is severe locally extensive necrosis of the epidermis, superficial dermis, and associated adnexa in some sections.
- Kidney: There is marked congestion and massive perivascular hemorrhage predominantly at the corticomedullary junction and variably throughout the cortex. Neutrophils frequently infiltrate the interstitium and multifocal blood vessel walls are thickened and hyalinized with many transmural neutrophils and frequent luminal fibrin thrombi. Multifocal glomerular capillaries are expanded and occluded by fibrin thrombi. Multifocal tubules are lined by degenerate to necrotic epithelia and lumens often contain sloughed cells, cellular debris, and occasional degenerate inflammatory cells.
- Spleen: The red pulp is variably expanded by many macrophages and moderate numbers of neutrophils.

Bacteriology:

- Routine culture: *Erysipelothrix rhusiopathiae* was isolated by culture from the spleen and kidney.
- *Erysipelothrix* IHC - positive on sections of skin, spleen, and kidney

Diagnosis: Acute swine erysipelas

Comment: Acute swine erysipelas (SE) occurs most often in pigs between 3 months and 3 years of age, and younger pigs are assumed to be protected by passive immunity; however, the pigs of this report were recently weaned and considerably younger than what is typical of acute SE. The characteristic 'diamond-skin lesions' often described with SE were not present in this case, and the vesicular lesions in one of the pigs were a curious finding (these tissues were negative for FMDV and CSFV by PCR). The distribution and appearance of the gross lesions was also somewhat reminiscent of PCV2 infection (PDNS); however, PCV IHC was negative on all tissues.

Reference:

Wood RL, Henderson, LM: 2006, Erysipelas. *In*: Diseases of swine, eds. Straw BE, Zimmerman JJ, D'Allaire STaylor DJ, 9th ed., pp. 629 - 638. Blackwell Publishing, Ames, IA.

Case #4

Focal symmetrical encephalomalacia in a goat

Francisco A. Uzal

California Animal Health and Food Safety laboratory, UCDavis,

San Bernardino Branch, California

Focal symmetrical encephalomalacia is the hallmark of chronic and sometimes sub-acute forms of *C. perfringens* type D enterotoxemia in sheep. However, this lesion is very rarely seen in type D enterotoxemia of goats. A 4 year old pigmy goat doe became ill with neurological signs, including pain to the touch and aggressive behavior (she bit the owner and attending veterinarian). Four days after disease onset the animal was presented to CAHFS for euthanasia and a full diagnostic work up. Grossly, the only significant lesions were many, firm, elevated, multifocal, white and chalky nodules (~ 2-3 mm diameter) in the pancreas. No significant gross abnormalities were seen in the brain. Histologically, in the brain there were well demarcated focal, bilateral and symmetrical lesions located in the midbrain (in the proximity of the occulomotor nuclei) and dorsal part of the pons, medial to the vestibular nuclei. These lesions consisted of degeneration and necrosis characterized by severe vacuolation of the white matter, with dilated myelin sheaths, axonal swelling (spheroids), neuronal necrosis, interstitial edema, diffuse microgliosis and presence of large, lipid-laden macrophages (Gitter cells). The astrocytes were hypertrophic, with large, vesicular nuclei and scant to moderate amount of eosinophilic cytoplasm. There was also hypertrophy of endothelial cells in both veins and arteries. The pancreas showed multifocal fat necrosis surrounded by granulomatous inflammation. This animal had severe skeletal and cardiac myopathy. No other significant histological abnormalities were observed in any of the multiple tissues examined. Vitamin E in liver was very low (this animal: 0.46 ppm; normal: > 3 ppm). Aerobic and anaerobic cultures of liver, lung and intestine, and heavy metal screen (including selenium) were unremarkable, except for isolation of large amounts of *C. perfringens* (not typed) from the colon. No parasite eggs were detected in feces, and rabies testing was negative. ELISA for *C. perfringen*s alpha, beta and epsilon toxins in intestinal content was negative. It is speculated that the brain lesion was produced by *C. perfringens* type D epsilon toxin and that the toxin could not be detected in intestinal content because of the chronicity of the process; the toxin having been washed away long before the necropsy was performed. There was probably no link between the brain lesion and the myopathy; the latter being consequence of vitamin E deficiency.

Case #5

Ligneous conjunctivitis in a Doberman pinscher

Alan T. Loynachan

Veterinary Diagnostic Laboratory, Department of Veterinary Science, College of Agriculture, University of Kentucky, Lexington, KY

Narrative: A four-year-old male neutered Doberman pinscher presented to its local veterinarian with a four-month history of bilateral conjunctivitis. The third eyelids and palpebral conjunctivae were reportedly covered by a pseudomembrane and were thickened, purple, proliferative, and friable. Schirmer tear tests were bilaterally normal. Conjunctivitis was unresponsive to systemic steroid administration and topical antimicrobial therapy. Surgical biopsies of the left conjunctiva and third eyelid were submitted to the University of Kentucky Veterinary Diagnostic Laboratory for histopathologic examination.

Histologically, lakes of small to moderate amounts of hyaline amorphous to fibrillar extracellular acidophilic proteinaceous material were multifocally deposited in the substantia propria and within the mucosal epithelium. Low to moderate numbers of lymphocytes, plasma cells, and neutrophils were intermixed with the proteinaceous material and aggregate in the superficial substantia propria. Large regions of the conjunctival epithelium had undergone squamous metaplasia, and there was mild to moderate squamous epithelial hyperplasia. There were rare foci of ulceration in the conjunctival epithelium, and low numbers of neutrophils and macrophages aggregated subjacent to the ulcers. Minimal numbers of neutrophils multifocally infiltrated the intact conjunctival epithelium and were located in occasional tarsal glands. Histochemically, the proteinaceous material was noncongophillic and stained variably Periodic acid-Schiff positive.

The combination of clinical history, gross description, and histopathology was consistent with a diagnosis of ligneous conjunctivitis.

Ligneous conjunctivitis is a rare chronic membranous conjunctivitis that is named based on the presence wood-like conjunctival membranes. The disease has been reported in dogs, mice, and humans. Doberman pinschers are the most commonly affected breed, but cases have also been reported in a Golden Retriever and a Yorkshire terrier.

Although the condition can be idiopathic, an underlying plasminogen deficiency has been identified in a number of human, murine, and canine cases. Plasmin(ogen) promotes wound healing by remodeling the fibrin-rich extracellular matrix (fibrin, plasma proteins, mucopolysaccharides, and immunoglobulins) deposited during wound stabilization. A lack of sufficient plasmin(ogen) inhibits remodeling and removal of the matrix, which results in the formation of the characteristic membranous lesions. Based on the underlying mechanism, systemic manifestations (alimentary, respiratory, reproductive, and urinary systems) can develop independently or in conjunction with the conjunctival lesions.

References:

McLean NS, Ward DA, Hendrix DV, et al.: 2008, Ligneous conjunctivitis secondary to a congenital plasminogen deficiency in a dog. J Am Vet Med Assoc 232:715-721.

Ramsey DT, Ketring KL, Glaze MB, et al.: 1996, Ligneous conjunctivitis in four Doberman pinschers. J Am Anim Hosp Assoc 32:439-447.

Schuster V, Seregard S: 2003, Ligneous conjunctivitis. Surv Ophthalmol 48:369-388.

Torres MD, Leiva M, Tabar MD, et al.: 2009, Ligneous conjunctivitis in a plasminogen-deficient dog: clinical management and 2-year follow-up. Vet Ophthalmol 12:248-253

Case #6

Pulmonary carcinosarcoma in a dog

Marie E. Pinkerton

Department of Pathobiological Sciences, University of Wisconsin-Madison, Madison, WI

A 9 ½-year-old, spayed female chocolate Labrador retriever was presented with an 8 to 12 week history of a non-productive cough. The dog was referred to the University of Wisconsin Veterinary Care clinic following thoracic radiographs, which showed a pulmonary mass. Additional thoracic radiographs and CT imaging localized the mass to the left cranial lung lobe. Cytology of a fine-needle aspirate of the mass showed neutrophilic and macrophagic inflammation, reactive fibroblasts, and tightly cohesive clusters of epithelial cells consistent with carcinoma. Thoracotomy and lung lobectomy were performed and the left lung lobe was submitted for histopathological examination. Tracheobronchial lymph nodes were not found at the time of surgery. Within the submitted lung was a 6.0 x 5.5 x 3.5 cm white firm mass at the base of the cranial portion of the left cranial lung lobe. The mass had a smooth pleural surface and was white to tan on section, variably firm, well demarcated, with few small pockets of tan mucoid material. Histologically, the mass was composed mostly of an epithelial population of cuboidal to columnar cells arranged in tubulopapillary structures, lobules, and trabeculae, with moderate anisocytosis and anisokaryosis. In addition, there were fewer areas in which the epithelial cells were separated by and confluent with streams of densely arranged spindle cells, with plump oval nuclei and no appreciable matrix. Broad areas of the mass were necrotic, and there were also lakes of mucin and suppurative inflammation. In one focus the mass appeared to be arising from or invading into a bronchus, filling the lumen (endobronchial growth). Immunohistochemistry showed strongly positive cytoplasmic labeling for both cytokeratin and vimentin in the spindle cell population, and the epithelial component was positive for cytokeratin and negative for vimentin. This was consistent with a pulmonary carcinosarcoma, a rare primary pulmonary neoplasm in animals and in humans. In humans these tumors are thought to arise from bronchial epithelium and often show endobronchial growth, as in this case. This neoplasm is typically aggressive in humans and has a poorer prognosis than other more common primary pulmonary tumors. Metastases can be composed of either one or both of the components. The dog was placed on weekly vinorelbine chemotherapy and monitored with periodic thoracic radiographs. Three months following thoracotomy, the dog was doing well with no signs of recurrence or metastasis.

.

References

Cupples J, Wright J. An immunohistological comparison of primary lung carcinosarcoma and sarcoma. Pathol Res Pract. 1990 Jun;186(3):326-9.

Ghisleni G, Grieco V, Mazzotti M, Caniatti M, Roccabianca P, Scanziani E. Pulmonary carcinosarcoma in a cat. J Vet Diagn Invest. 2003 Mar;15(2):170-3.

Salas G, Román O, Gutiérrez Díaz-Ceballos ME, Constantino F. Lung carcinosarcoma in a dog: gross and microscopic examination. Vet J. 2002 May;163(3):331-4.

Thomas VT, Hinson S, Konduri K. Epithelial-mesenchymal transition in pulmonary carcinosarcoma: case report and literature review. Int Surg. 2006 Jan-Feb;91(1):28-32.

Case #7

Hypereosinophilic Syndrome in a Domestic Shorthaired Cat

Jeremy Tobias, Luke Borst

North Carolina State University College of Veterinary Medicine

Signalment: 11-year-old, spayed female, 4.2 kg, domestic shorthaired cat

Clinical History: The patient initially presented to the NCSU Internal Medicine service for inappropriate urination and was seen episodically over the course of 2 months. Additional clinical signs noted included fever (103.7^{o} F), tachycardia, hematochezia, and ultimately, tachypnea, open-mouth breathing, and cardiac arrest. CBC findings included a normocytic, normochromic anemia (PCV 25%) and a progressive leukocytosis (up to 51,630/ul), characterized by a marked eosinophilia (25,586/ul) and moderate mature neutrophilia (36,940/ul). Radiographs and ultrasound revealed a diffusely infiltrated small intestinal wall, lymphadenomegaly, and progressive bronchial pattern with inflammatory nodules. Jejunal lymph node aspiration and transtracheal wash revealed severe eosinophilic infiltrates. Bone marrow aspiration yielded an M:E ratio of 1.46 and moderate-marked eosinophil hyperplasia. Additional etiologies investigated with negative results include: FIV/FeLV, dirofilariasis, intestinal parasitism, toxoplasmosis, *Bartonella hensalae/vinsonii*, mycoplasmosis, bacteremia, and lymphoid neoplasia.

Gross Description: The lungs are diffusely rubbery, fail to collapse and have clearly visible rib impressions. The right middle and accessory lobes are diffusely mottled pink to red, while the remaining lobes contain map-like foci of red mottling. On cut surface of the left caudal lobe, there is a 0.05-0.1 cm thick rim of peribronchial pallor.

Microscopic Description: The lungs contain a marked, multifocal to coalescing, peribronchiolar and perivascular infiltrate of mature eosinophils, which extend into the airways and obscure the adjacent parenchyma. Bronchioles are lined by a moderately increased number of glands and large airways are frequently filled with abundant mucous mixed with many eosinophils and sloughed epithelial cells. Throughout the section the bronchioles and terminal bronchi are supported by increased smooth muscle. Multifocally alveoli frequently contain foamy macrophages and hemorrhage. The alveolar septa are hypercellular with numerous circulating eosinophils and frequent megakaryocytes. Other organs infiltrated by mild to moderate numbers of eosinophils include: bone marrow, lymph nodes, spleen, stomach, ileum, liver, and kidney.

Diagnosis: 1) Lung: marked, diffuse perivascular and peribronchial eosinophilic bronchointerstitial pneumonia (with multiorgan eosinophilia consistent with idiopathic hypereosinophilic syndrome)

2) Lung: marked, diffuse bronchial gland hyperplasia with smooth muscle hypertrophy and intralumenal mucous (consistent with feline asthma)

Comment: Extensive, multi-organ eosinophilic inflammation like that observed in this patient can be classified into to 3 broad categories; reactive eosinophilia, chronic eosinophilic leukemia (CEL) or hypereosinophilic syndrome (HES). Several changes present in this patient are consistent with feline asthma which is frequently associated with reactive eosinophilia; however, the large quantity of eosinophilic infiltrates was considered atypical. As such, CEL and HES were considered. Evidence supporting CEL includes a circulating neutrophil population that outnumbers the eosinophils, a moderate anemia, and the relatively quick clinical course following initial diagnosis. On the other hand, evidence supporting HES is the lack of a prominent blast population within the bone marrow or circulating blood, a myeloid:erythroid ratio less than 10:1, and a relatively low total circulating leukocyte count. In conclusion, we prefer the diagnosis of feline asthma complicated by systemic hypereosinophilic syndrome in this patient.

References: Valli. Veterinary Comparative Hematopathology. 2007. P436-440.

Case #8

Feline Endomyocarditis and Interstitial Pneumonia

Linden Craig, DVM, PhD, DACVP

Department of Biomedical and Diagnostic Sciences

University of Tennessee College of Veterinary Medicine

Signalment: 13 year old neutered male domestic long hair cat

Clinical History: This cat had an eight month history of intermittent diarrhea with blood which was treated for Giardia with no response. Acute respiratory distress began 2 days ago. Echocardiogram was consistent with hypertrophic cardiomyopathy. Radiographs were suggestive of heart failure. There was minimal response to treatment. Owner elected euthanasia.

Gross Findings: The heart was enlarged (24.8g, 0.59% of body weight; normal is 0.3-0.45%) and the left auricle was dilated (larger than the right). The lungs were wet and heavy. The trachea and bronchi contained abundant white foam. The small intestinal wall was multifocally thickened and the mesenteric lymph nodes were enlarged.

Microscopic Description: Heart, interventricular septum: The endocardium is thickened, especially on the left side, by fibrin, hemorrhage, granulation tissue, and inflammatory cells. The inflammatory cells are mostly neutrophils, with fewer eosinophils, macrophages, and lymphocytes. The interstitium of the adjacent myocardium is infiltrated and expanded by plump fibroblasts, erythrocytes, and inflammatory cells. There is degeneration of the affected myocardiocytes characterized by vacuolation and loss of striations.

Lung: Alveolar spaces contain increased numbers of macrophages as well as fibrin, edema fluid, and red blood cells. Alveolar septa are thickened by congested capillaries, karyorrhectic debris, and rare type II pneumocyte hyperplasia.

Diagnosis: Feline endomyocarditis with interstitial pneumonia

Comment: Feline endomyocarditis is an idiopathic condition which frequently follows a period of stress (e.g. surgery, illness, change in household). In most cases there is an associated interstitial pneumonia and most cats present in respiratory distress. It is thought to be caused by recrudescence of a latent infection that targets the endothelial cells of the heart and lung. The cause is unknown and treatment is usually ineffective. The diagnosis can only be made postmortem. The left ventricular outflow tract (left side of the interventricular septum) is typically the most severely affected area and should be examined microscopically in all cats submitted for necropsy. The lesion is often not apparent grossly. Rarely, cats survive the acute phase of the disease and go on to develop left ventricular endocardial fibrosis (restrictive cardiomyopathy).

The diarrhea and thickened small intestinal segments were caused by intestinal lymphosarcoma, which was presumably the stress that precipitated the endomyocarditis in this case.

References:

1. Stalis IH, Bassbaly MJ, Van Winkle TJ. Feline endomyocarditis and left ventricular endocardial fibrosis. *Veterinary Pathology* 32:122-126, 1995

2. Maxie MG, Robinson WF. Cardiovascular system. *In:* Jubb, Kennedy, and Palmer's Pathology of Domestic Animals, ed. Maxie MG, pp. 46-47. Saunders Elsevier, Philadephia, PA, 2007.

Case #9

Arthrogryposis and myelodysgenesis in a calf with evidence of *in utero* Schmallenberg virus infection

Sandra Scholes[1], Susanna Williamson[2], Falko Steinbach[3]

[1]Animal Health Veterinary Laboratories Agency (AHVLA) Lasswade, Pentlands Science Park, Penicuik, Midlothian EH26 0PZ, Scotland

[2]AHVLA Bury St Edmunds

[3]AHVLA Weybridge

This full term deformed calf was the only such submission from a beef suckler herd of 30 to 40 breeding cows. The calf was shot. The cattle grazed on fields neighboring a sheep flock under different ownership in which Schmallenberg virus (SBV) infection was confirmed in malformed lambs.

Necropsy examination revealed a circular full-thickness skin defect in the cranium where the calf had been shot and the whole skull and top jaw were extensively fractured with widespread soft tissue damage associated with the method of euthanasia. Both forelimbs were partially flexed; both could be flexed further but could not be further extended. Both hindlimbs had fixed flexion of the hip, stifle and hock joints. There was slight flexion of the neck to the left. Lumbar axial and bilateral hindlimb musculature was poorly developed and cut surfaces were gelatinous and homogeneous. Micromyelia involved particularly the lumbosacral intumescence; differentiation between ventral horn and adjacent funiculi was not detectable on cut surfaces and the regions of the lateral and ventral funiculi were darker than the dorsal funiculus. Histological examination of the spinal cord revealed small ventral horns bilaterally containing very few or no neuronal cell bodies and lack of demarcation between the ventral horn and adjacent hypomyelinated ventral and lateral funiculi. The ventral spinal nerve roots were markedly small compared with the dorsal spinal nerve roots and the connective tissue of the ventral median fissure was prominent. There was an impression of a reduction in the numbers of ventral horn neurones at the cervical intumescence, and many of the neurones were angular, and an impression of asymmetry in the number of ventral horn neurones at cervical segment 3. Examination of remaining portions of brain revealed focal cerebrocortical dysplasia with marked thinning of cortex, laminar disorganisation and occasional basophilic structures consistent with mineralised neurones with sparse lymphohistiocytic infiltrate in overlying meninges. The reduction in number of ventral horn neurones is a plausible explanation for decreased limb movement *in utero* and consequent development of arthrogryposis.

Schmallenberg virus nucleic acid was not detected by PCR in multiple samples including brain (cerebral cortex), cervical spinal cord and spleen. SBV antibody was detected in serum.

The character and distribution of the spinal cord lesions in this calf are distinct from those associated with *in utero* BVDV and BTV-8 infections. The lesions are similar to those occurring in calves and lambs associated with *in utero* infection with other orthobunyaviruses, such as Akabane and Cache Valley viruses, and in arthrogrypotic lambs in which SBV sequences have been detected. Similarly, the presence of an antibody response and the lack of detectable virus are also features of Akabane virus-associated arthrogryposis in calves.

Case #10

Pararenal Myelolipomas in a Commercial Flock of Egg-laying Hens

Allison Boone, Michael Martin, H. John Barnes

College of Veterinary Medicine, North Carolina State University, Raleigh, NC

Signalment and Clinical History: Nine of one hundred three, clinically healthy, 102-116 weeks old, HyLine W36 laying hens from a flock on a commercial, multi-age laying farm in eastern North Carolina comprised of 80,000 hens housed in conventional A-frame cages had pararenal myelolipomas. The flock was at the end of their second laying cycle. Production, morbidity, and mortality for the flock were within expected limits and the flock had experienced no significant health issues.

Gross Description: Single to multiple, soft, tan to pink to light red, variably sized tumors were located within the potential space between the caudal division of the kidney and caudal renal fossa of the synsacrum. Tumors did not invade or compress adjacent kidneys or bone, but large tumors displaced the caudal division of the kidney ventrally. Smaller tumors were freely embedded in adipose tissue.

Microscopic Description: All tumors were similar histologically and consisted of a variable mixture of hematopoietic (erythroid and myeloid), lymphoid, and mature adipose cells. Hematopoietic cells consisted of extra-sinusoidal granulocytes ranging from myeloblasts to mature granulocytes, immature to mature erythrocytes within sinusoids, and hemocytoblasts. Rare mitotic figures were observed. Tumors were not invasive.

Diagnosis: Pararenal Myelolipomas

Comment: Myelolipomas occur in human beings as well a variety of animals, both mammalian and avian. The incidence of myelolipomas is infrequent in animals compared to humans. In people, tumors occur most commonly in the adrenal glands; however, other locations have been reported. The average age at diagnosis in people is approximately 50 years, and most patients are asymptomatic, but flank pain or hematuria has been reported. In animals, tumors have been reported in dogs, domestic and exotic cats, nonhuman primates, cattle, and a ferret, and have been observed in the liver, spleen, adrenal gland, abdominal cavity (greater omentum), and spinal epidural and extradural regions. There are no specific clinical signs and the tumors can be single or multiple and considered benign. In birds, tumors have been reported in geese, lovebirds, saffron toucanet, society finch, hyacinth macaw, and a cockatiel, and have been observed in the liver, and cutaneous, subcutaneous, and thoracoabominal locations. To our knowledge, myelolipomas have not been reported in poultry. This report documents myelolipomas in laying hens, which were found to be in an unreported location, between the kidney and synsacrum. Prevalence is currently unknown and although the lesions do not appear to be clinically significant, they should not be mistaken for lesions that would negatively impact the birds or productivity of the flock.

References: Hatai H, Ochiai K, Nakamura S, et al.: 2009, Hepatic Myelolipoma and Amyloidosis with Osseous Metaplasia in a Swan Goose (*Anser cygnoides*). J Comp Path 141: 260-264
Kamiie J, Fueki K, Amagai H, et al.:2009, Multicentric Myelolipoma in a Dog. J Vet Med Sci 71:371-373.
Lack EE, Wieneke JA: 2010, The Adrenal Glands. *In:* Sternberg's Diagnostic Surgical Pathology, ed. Mills SE, Volume II, pp.562-563. Wolters Kluwer Health/Lippincott Williams & Wilkins, Philadelphia, PA.

Newman SJ, Inzana K, Chickering W, et al.: 2000, Extradural Myelolipoma in a Dog. J Vet Diagn Invest 12: 71-74.
Ozaki K, Kinoshita H, Kurasho H, et al.: 1996, Cutaneous myelolipoma in a peach-faced lovebird (*Agapornis roseicollis*). Avian Pathol 25: 131-134.

Case #11

Canine parvoviral infection and Salmonellosis

Mahogany W. Caesar, Peter Moisan and Karen Post

Rollins Animal Disease Diagnostic Laboratory, Raleigh, North Carolina

Signalment and History: A 12-week-old male Whippet puppy developed profuse hemorrhagic vomiting and diarrhea with leukopenia. The canine parvovirus ELISA test was negative. The puppy failed to respond to supportive therapy and was euthanized. Five littermates were treated concurrently for similar clinical signs. Canine parvoviral enteritis was suspected. These puppies were current on the canine distemper-parvovirus vaccine, routinely dewormed and fed a commercial raw food diet.

Gross examination: This male Whippet puppy weighed 6 kg with thin body condition and moderate dehydration. The small intestinal, cecal and colonic mucosa was diffusely lined by a thick fibrinous pseudomembrane.

Morphologic diagnoses:

- Small intestine; crypt degeneration and necrosis, segmental, severe with epithelial regeneration and lymphofollicular atrophy
- Small intestine and colon; enterocolitis, fibrinosuppurative, multifocal, moderate to severe with intralesional bacilli and coccidial forms

Immunohistochemistry: There is immunoreactivity to canine parvovirus antigen in the small intestine and tongue.

Bacteriology: 2+ *Salmonella* sp. (does not group) isolated in the small intestines.

Salmonella serotyping: *Salmonella enterica* serotype *newport*

Diagnosis: Canine parvoviral enteritis and Salmonellosis

Comments: *Salmonella newport* is of considerable animal and public health concern as it causes significant clinical disease in livestock (especially cattle), humans and other animal species. This serotype has been recovered from contaminated dog foods, treats and chews made from bovine and poultry products. Multiple antimicrobial resistant strains of *S. newport* have been recorded. The commercial raw food is the suspected source of salmonellosis. Persistence and severity of salmonella infection depends on the patient's immune status, which is compromised in this case due to the canine parvoviral infection. Interestingly, *Salmonella newport* was also detected in the feces from one of the five hospitalized puppies. Canine parvovirus-2 (CPV-2) typically causes gastroenteritis and is associated with high morbidity and mortality. False-negative results can occur with the canine parvovirus ELISA in early stages (prior to fecal shedding) or late stages (virus has become bound to specific antibody); therefore a negative result does not rule out the disease. The shed window for CPV is typically highest day 4 to day 14 post exposure.

References:

1. www.addl.purdue.edu; Newsletter 2004. Salmonella Newport – An emerging disease in dairy cattle.
2. USDA/APHIS "What veterinarians and producers should know about multidrug-resistant Salmonella Newport" information sheet; September 2002
3. IDEXX website: www.idexx.com; FAQ section
4. Jubb KVF, Kennedy PC, Palmer: Pathology of Domestic Animals 5th ed., vol. 2, pp. 193-195

Case #12

Canine distemper virus, canine adenovirus virus type 2, and *Mycoplasma* pneumonia in a Dog

Jenny Bernard, Julia Lankton, and Robert Donnell

Department of Biomedical and Diagnostic Sciences, College of Veterinary Medicine, University of Tennessee, Knoxville, TN 37996

Signalment and history: This was a four week old male Labrador retriever puppy from a litter of nine rescue puppies from Alabama. Puppies were emaciated, weak, and had nasal and ocular discharge. This was the fourth puppy to die; necropsies were not performed on the other animals. Treatment included steroid administration seven days prior to this puppy's necropsy.

Gross lesions: Predominantly within the cranioventral lung lobes but affecting all lobes, there were multifocal to coalescing 3-10 millimeter diameter tan nodules which, on cut section, contained thick opaque yellow fluid. The caudal lung lobes were rubbery and failed to collapse. All lung sections sank in formalin. The tracheal mucosa was diffusely coated with opaque brown fluid. Other gross findings included a poor body condition, sunken eyes, mild catarrhal rhinitis, and thin purulent yellow to tan material within the left tympanic bulla.

Histopathology and immunohistochemistry: Multifocally filling bronchi, bronchioles, and alveoli are marked infiltrates of neutrophils mixed with fewer macrophages, fibrin, and karyorrhectic debris. There is multifocal type II pneumocyte hyperplasia, hyaline membrane formation, and alveolar necrosis. Pneumocytes, macrophages, and bronchial, bronchiolar and peri-bronchial gland epithelium frequently contain 5-10 micrometer amphophilic intranuclear inclusions with marginated chromatin (adenovirus inclusions). Rarely, there are 2-4 micrometer eosinophilic cytoplasmic inclusions predominantly within bronchial gland epithelium (distemper virus inclusions). There is variable hyperplasia and necrosis of the bronchial, bronchiolar and bronchial gland epithelium. Bronchi and blood vessels are surrounded by lymphocytes and plasma cells. Immunohistochemical stains highlight abundant canine distemper virus antigen within bronchial and bronchiolar epithelium, bronchial gland epithelium, and macrophages, as well as canine adenovirus antigen predominantly within macrophages.

Additional diagnostic testing: Polymerase chain reaction (PCR) was positive for canine distemper virus (CDV), canine adenovirus type 2 (CAV2), and *Mycoplasma* on fresh and frozen lung samples taken postmortem. Postmortem cultures of lung isolated greater than 500 colonies *Mycoplasma* spp. PCR was negative for *Bordetella bronchiseptica*, canine herpes virus 1, influenza A, canine parainfluenza virus type 3, canine respiratory coronavirus, and canine coronavirus.

Comments: CDV most commonly affects dogs 12-16 weeks of age due to waning passive immunity and exposure to subclinically infected dogs. This *Morbillivirus* is known for causing immunosuppression that leads to secondary infections. In this case, necrotizing bronchointerstitial pneumonia is attributed to primary infection with CDV with secondary infection with CAV2 and suppurative bronchopneumonia from *Mycoplasma* spp. There are few case reports of dual infections with CAV2 and CDV, and one report of all three agents contributing to pneumonia in a dog. Additional histologic findings in this case included splenic lymphoid depletion (attributed to CDV), and multifocal biliary and hepatic necrosis with adenoviral inclusions in periportal hepatocytes, Kupffer cells, and biliary epithelium. There were no gross or microscopic lesions in the brain.

References:

1. Chvala S., et al. 2007. Simultaneous canine distemper virus, canine adenovirus type 2, and *Mycoplasma cynos* infection in a dog with pneumonia. *Vet Pathol* 44:508-512.
2. Damián M., et al. 2005. Immunohistochemical detection of antigens of distemper, adenovirus and parainfluenza viruses in domestic dogs with pneumonia. *J Comp Path* 133:289-293.

Case #13

Brucella canis-associated placentitis and abortion in two puppies

Jeffrey R. Hayes, Craig Sarver, Jing Cui, Yan Zhang, Anne Parkinson, Beverly Byrum
Ohio Department of Agriculture, Animal Disease Diagnostic Laboratory, Reynoldsburg, Ohio

Signalment: Two Labradoodle fetuses, one male and one female

Clinical History: The dam expelled six fetuses at 56 days gestation. Two of the fetuses were presented to the ADDL for necropsy and ancillary testing.

Gross lesions: The male fetus was 15cm crown to rump, had no hair, and the lungs were non-aerated, dark pink and slightly firm. The rest of the viscera, brain and placenta had no gross lesions that could be differentiated from moderate autolysis. The female fetus was 8cm crown to rump, leathery gray skin, and tissues were tannish gray and clay-like. The placenta was severely autolytic.

Ancillary test results: Heavy growth of *Brucella canis* was isolated from fresh placenta; moderate growth of *B. canis* was also isolated from lung and liver of the male fetus. No other pathogenic bacteria or viruses were detected by ancillary tests.

Histopathology:
Placenta: There are multiple discrete and occasionally coalescing areas of coagulation necrosis in the stroma of the chorioallantois, evidenced by hypereosinophilia and loss of differential staining, accompanied by focal infiltration of the stroma by non-degenerate neutrophils. There are also regions containing degenerate neutrophils admixed with abundant pyknotic and karyorrhectic debris. Scattered trophoblastic epithelial cells also contain hypereosinophilic cytoplasm (necrosis), but most appear viable and are distended by myriad punctate basophilic to amphophilic structures within the cytoplasm (intracytoplasmic bacteria). Aggregates of brown granular to globular material are also present on the surface (meconium).

Morphologic Diagnoses:
Placenta: Marked multifocal to coalescing acute necrotizing placentitis with intracytoplasmic bacteria

Discussion: *Brucella canis*, a small Gram negative, aerobic coccobacillus, has been recognized as a cause of canine reproductive disease since 1966. Transmission of the organism often occurs by oronasal contact with vaginal secretions and aborted materials; shedding of the organism by the dam is known to occur up to 6 weeks after abortion. Transmission via the dam may also occur in utero or through ingestion of the dam's milk. Histologically there was focal neutrophilic fetal pneumonia in the lung of the male fetus, with isolation of moderate growth of *B. canis* from fresh lung tissue. Aspiration of contaminated amniotic fluid likely occurred secondary to placentitis, disruption of maternal/fetal oxygen exchange, fetal hypoxia and deep inspiration of bacteria in the fluid. Transmission via male dogs may occur by seminal fluids and urine; fomite transmission has also been reported to occur. This organism can cause human illness, including signs of fever, chills, fatigue, lethargy, weight loss, lymphadenopathy, conjunctivitis, uveitis, polyarthritis and spondylitis.

References:
1. Foster, RA. Female reproductive system and mammary gland. In: Zachary and McGavin's Pathologic Basis of Veterinary Disease, 5th edition, ed. Zachary JF and McGavin MD, p 1117. Elsevier Mosby, St. Louis, MO. 2012.
2. Lopez A. Respiratory system, mediastinum and pleurae. In: Zachary and McGavin's Pathologic Basis of Veterinary Disease, 5th edition, ed. Zachary JF and McGavin MD, p 531. Elsevier Mosby, St. Louis, MO. 2012.
3. Schlafer, DH, Miller RB. Female genital system. In: Jubb, Kennedy, and Palmer's Pathology of Domestic Animals, dition, ed. Maxie MG, pp. 484-489. Saunders Elsevier, Philadelphia, PA, 2007.

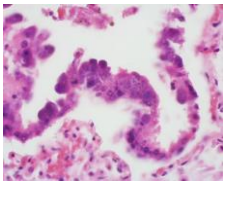
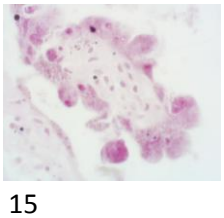

Case #14

Selenium Toxicosis in a Commercial Swine Operation

K.M. Almes, A.G. Cino-Ozuna[1], P.S. Malhi[1], S.C. Henry[2], L.M. Tokach[2], D. van der Merwe[1],

1. Kansas State Veterinary Diagnostic Laboratory, Kansas State University, Manhattan, KS
2. Abilene Animal Hospital, Abilene, KS

Signalment: three approximately 14-week-old finisher pigs submitted live

History: The pigs originated from a farm with a history of feed refusal, hind limb paresis, and lameness. On physical examination, the three pigs had retained proprioceptive responses in both hind limbs, responded to deep pain, were unable to rise on the rear limbs, and exhibited bruxism and hypersalivation. Gross necropsy revealed bilaterally symmetric areas of poliomyelomalacia within the ventral horns of the cervicothoracic and lumbosacral spinal cord regions.

Laboratory Findings: Screening for mycotoxins and pesticides were negative. Elevated levels of selenium were detected in tissues from 2 of the pigs and whole blood from 1 of the pigs (liver- 5.66ppm & 9.04ppm; reference range toxic >3ppm, kidney- 5.57ppm & 6.59ppm; reference range toxic >3.8ppm; whole blood 12.77ppm; reference range toxic .08-.35ppm). The trace mineral premix supplement used in the mixed ration contained up to 4600 ppm of selenium (expected value: 198 ppm), indicating this was the source of the toxicosis.

Histopathology Findings: Spinal cords from all 3 pigs displayed bilaterally symmetrical poliomyelomalacia characterized by vacuolation of the neuropil, multifocal neuronal necrosis, multifocal gliosis, infiltration by large numbers of gitter cells, and variable lymphoplasmacytic perivascular cuffing often surrounding vessels that were lined by plump reactive endothelial cells.

Final Diagnosis: A diagnosis of selenium toxicosis was made based on the clinical signs, characteristic histopathologic lesions, and toxic levels of selenium found in the liver, kidney, and whole blood. This was further supported by the markedly elevated levels of selenium detected in the trace mineral premix fed on this farm.

Comments: Another 292 finisher pigs and 37 sows died or were euthanized with similar clinical signs and hoof lesions. About 14,000 grower pigs were exposed to the toxic levels of selenium in the premix, but most showed no clinical signs. Chronic selenium toxicosis is characterized by bilaterally symmetrical focal poliomyelomalacia, hair loss, sloughing of hooves, and hepatic and renal degeneration in pigs.[1] Selenium toxicosis is rarely seen in large swine operations, with commercially prepared diets, but when identified, it is typically the result of a calculation error in feed formulation, as in this case.

References: 1. Carson TL. Toxic Minerals, Chemicals, Plants, and Gases. In: Straw BE, Zimmerman JJ, D'Allaire S, Tayler DJ, eds. *Diseases of Swine*. 9th ed. Ames, IA.

Case #15

Fourth Ventricular Cystic Mass in a Dog

Gayle Johnson, Sean Spagnoli, Fred Wininger, Kei Kuroki, Melanie Spoor

Work from the University of Missouri Department of Veterinary Medicine and Surgery (Wininger) and Veterinary Medical Diagnostic Laboratory (Spagnoli, Kuroki, Spoor and Johnson)

A 3 year old neutered female mixed breed dog was presented for evaluation of cervical pain and a head tilt. Computerized tomography revealed a cystic mass in the left cerebellar-medullary recess. The mass was incompletely excised by suboccipital craniotomy, and despite full recovery from anesthesia, the patient expired 3 hours after surgery. At postmortem, a mass was present to the left of the cerebellar vermis. The mass was associated with the fourth ventricular choroid plexus, and extended from the middle cerebellar peduncle to the level of the olives in the medulla. The mass indented the brain and was a large cyst lined segmentally by viable keratinizing epithelium. The epithelium consisted of basal, spinous and granular layers with a central lumen containing multilayered keratin squames. Epithelial layers were supported by fibrous tissue, and neither rete pegs nor adnexa were present. Much of the cyst was effaced by hemorrhage and by formation of granulomas containing numerous acicular clefts. Localized granulomatous and lymphocytic inflammation was present in the meninges and in subarachnoid space of nearby brain, especially where keratin squames were present in the subarachnoid space. Considerable recent hemorrhage was present along the base of the brain, extending to the optic chiasm, and in the lumen of the third ventricle. A diagnosis of epidermoid (keratinous) cyst was made. Shortly after neural tube closure during development, the fourth ventricular choroid plexus forms by invagination of mesenchyme-derived epithelial tissue into the nascent brain. Cysts such as these are presumed to arise from attached ectodermal tissue that becomes embedded in the stroma as the choroid plexus forms. Most of keratinous cysts in dogs are associated with choroid plexus, and rarely keratoacanthomas or squamous cell carcinomas may arise from them or at least occupy a similar anatomical location. In dogs, most cysts have been reported from the cerebellopontine angle and fourth ventricle, with secondary compression of the medulla oblongata and cerebellum causing neurologic dysfunction. Younger dogs are usually affected. Less commonly they are observed in the spinal cord, also of young dogs. In the spinal cord lesions of humans, previous neurosurgery or spinal tap are thought to possibly introduce epidermal tissue that subsequently proliferates. Keratinous cysts are entirely similar to epidermal cysts found in skin. These growths have benign course when completely removed but can regrow if incompletely excised. In addition, pre- or post surgical rupture can cause acute or chronic chemical meningitis, as occurred in this case.

Kornegay JN, Gorgacz EJ. Intracranial epidermoid cysts in three dogs. Vet Path 1982 Nov;19(6):646-50.

Lipitz L, Rylander H, Pinkerton ME. Intramedullary epidermoid cyst in the thoracic spine of a dog. J Am Anim Hosp Assoc. 2011 Nov-Dec;47(6):e145-9.

Spoor MS, Spagnoli ST, Burton E, Romsland RD, Wininger FA, Kuroki K, Wiedmeyer CE. What is your diagnosis? Cystic mass in the fourth ventricle of a dog (Epidermoid cyst). Vet Clin Pathol. In press.

Case #16

Exfoliative Dermatitis of the German Shorthaired Pointer

Elisa Salas

Resident, Veterinary Anatomic Pathology

University of Nebraska-Lincoln

Signalment: 6-month-old male castrated German shorthaired pointer.

Clinical History: Alopecia and mild crusting beginning at the ear tips were first noted by the owner at 4 months of age. Signs progressed to the dorsum of the nose, ventral abdomen, caudal thighs and the patient became pruritic. Skin scrapings were negative and there was no response to therapy.

Microscopic description: Sections of skin are characterized by mild multifocal epithelial apoptosis, scattered interface inflammation, apoptosis of follicular epithelium, and perivascular superficial dermatitis. Epidermis and follicular epithelium are affected by civatte body formation is present in the stratum basale, and less so in the stratum spinosum and in the follicular wall. Also seen is mild exocytosis of lymphocytes. Multifocally obscuring the epithelium are infiltrates of few to moderate lymphocytes. Mild amounts of lymphocytes and plasma cells are seen in the superficial dermis, surrounding blood vessels. Additionally, there is rare dermoepidermal clefting, moderate multifocal pigmentary incontinence, and mild orthokeratosis.

Morphologic Diagnosis: Haired skin: Mild, multifocal, chronic, lymphocytic interface dermatitis with apoptosis

Comments: Differentials considered were discoid lupus erythematosis, systemic lupus erythematosis, exfoliative dermatitis of German short-haired pointers, mucocutaneous pyoderma, erythema multiforme, and lupoid drug reaction. Recent work identifies this condition as having autosomal recessive inheritance due to a singular nucleotide polymorphism of an as-of-yet unidentified gene on chromosome 18. Females and young dogs are overrepresented. Clinical signs, ordered from greatest to least include scaling, alopecia, crusting with or without ulceration, generalized lymphadenopathy, follicular casts, mild pruritus, and intermittent pyrexia. These affect the muzzle, pinnae, dorsal trunk and progress in 52% of patients to the limbs and ventral trunk. Noncutaneous findings consisted of peripheral lymphadenopathy, colitis, eosinophilic and lymphoplasmacytic enteritis, shifting-leg progressive lameness, and infertility. Most patients are euthanized due to lack of response to therapy or effects of immunosuppression.

References

1. Bryden SL, White SD, Dunston SM et al. Clinical, histopathological and immunological characteristics of exfoliative cutaneous lupus erythematosus in 25 German short-haired pointers. *Veterinary Dermatology* 2005; 16: 239–52.
2. Gross TL, Ihrke PJ, Walder EJ. Hereditary lupoid dermatosis of the German Shorthaired Pointer. In: *Veterinary Dermatopathology: a Macroscopic and Microscopic Evaluation of Canine and Feline Skin Diseases*. St Louis: Mosby Year Book, 1992: 26–8.
3. Gross TL, Ihrke PJ, Walder EJ, Affolter VK. Exfoliative cutaneous lupus erythemaosus of the German shorthaired pointer. In: *Skin diseases of the Dog and Cat: Clinical and Histopathologic Diagnosis*. 2nd ed. Ames, IA. Blackwell Science; 2005: 59-61 and 65-68.
4. Mauldin EA, Morris DO, Brown DC, Casal ML. Exfoliative cutaneous lupus erythematosus in German shorthaired pointer dogs: disease development, progression and evaluation of three immunomodulatory drugs (ciclosporin, hydroxychloroquine, and adalimumab) in a controlled environment. *Vet Dermatol*. 2010; 21(4):373–382.
5. Wang P, Zangerl B, Werner P, Mauldin EA, Casal ML. Familial lupus erythematosus (CLE) in the German shorthaired pointer maps to CFA18, a canine orthologue to human CLE. *Immunogenetics*. 2011; 63 (4) 197-207.

Case #17

Bacterial pseudomycetoma in a Chinese hamster (*Cricetulus griseus*)

Marcia R. S. Ilha

University of Georgia, Tifton Veterinary Diagnostic and Investigational Laboratory, 43 Brighton Road, Tifton 31793

Signalment: young adult, male, Chinese hamster (*Cricetulus griseus*)

Clinical history: Formalin-fixed tissues were received from a Chinese hamster with a clinical history of a firm swelling under the left eye that was attached to the maxilla. The hamster had been treated for ocular disease 3 weeks prior to the biopsy. Two other hamsters from the same group of animals developed similar sub-ocular swellings. In one of the affected animals the swelling was an abscess. Fresh samples were not submitted for bacterial culture. These animals were from a pet store.

Histopathology: Hematoxylin & eosin and gram stained sections of subcutaneous tissue, skeletal muscle, and bone were examined. Affecting these tissues there were multifocal to coalescing pyogranulomas. These pyogranulomas were characterized by central large bacterial colonies of gram-positive cocci surrounded by a rim of eosinophilic radiating and clubbed material (Splendore-Hoeppli reaction) and numerous neutrophils and histiocytes. Pyogranulomas were separated by fibrovascular tissue infiltrated by plasma cells and lymphocytes.

Morphologic diagnosis: Marked pyogranulomatous panniculitis, myositis and osteomyelitis with intralesional gram-positive bacterial colonies of cocci (bacterial pseudomycetoma)

Comments: The lesion was histologically consistent with bacterial pseudomycetoma and resembles the lesion seen with botryomycosis due to *Staphylococcus* spp. Reports of similar lesions are described in dwarf hamsters (*Phodopus sungorus*),[1,3] Roborovski hamster (*Phodopus roborovskii*)[2] and rats[4]. In one report *Staphylococcus intermedius* was isolated from the lesions.[2] In affected hamsters lesions have been described as multifocal affecting nose, mouth,[1] single or multiple distal limbs and paws.[1,2,3]

References:

1. Eshar D, Mayer J, Keating JH. Dermatitis in a Siberian hamster (*Phodopus sungorus*). Bacterial pseudomycetoma. Lab Anim. 2010, 39 (3): 71-73.
2. Lee SY, Yoo JH, Park HM, Kim DY. Pathology in practice. Bacterial pseudomycetoma. J Am Vet Med Assoc. 2011, 239 (5): 583-585.
3. Martorell J, Gallifa N, Fondevila D, Rabanal RM. Bacterial pseudomycetoma in dwarf hamster, *Phodopus sungorus*. Vet Dermatol. 2006, 17 (6): 449-452.
4. Percy DH, Barthold S. Pathology of Laboratory Rodents and Rabbits, 2007, 3rd ed. Blackwell Publishing, Ames, p. 149.